Insights into the ion-coupling mechanism in the MATE transporter NorM-VC

Krah, Alexander; Zachariae, Ulrich

Published in:
Physical Biology

DOI:
10.1088/1478-3975/aa5ee7

Publication date:
2017

Document Version
Peer reviewed version

Insights into the ion-coupling mechanism in the MATE transporter NorM-VC

Alexander Krah[1,2,*] & Ulrich Zachariae[1,2]

[1]Computational Biology, School of Life Sciences, University of Dundee, Dundee, DD1 5EH, UK
[2]Physics, School of Science and Engineering, University of Dundee, Nethergate, Dundee, DD1 4NH, UK

*Corresponding author. E-mail: alexkrah@kias.re.kr

Key words: MATE transporter, MD simulations, antimicrobial resistance

Abstract

Bacteria have developed a variety of different mechanisms to defend themselves from compounds that are toxic to them, such as antibiotics. One of these defence mechanisms is the expulsion of drugs or other noxious compounds by multidrug efflux pumps. Multidrug and toxic compound extrusion (MATE) transporters are efflux pumps that extrude metabolic waste and a variety of antibiotics out of the cell, using an ion gradient as energy source. They function via an alternative-access mechanism. When ions bind in the outward facing conformation, a large conformational change to the inward facing conformation is induced, from which the ion is released and the extruded chemical compound is bound. NorM proteins, which are usually coupled to a Na^+ gradient, are members of the MATE family. However, for NorM-VC from *Vibrio cholerae*, it has been shown that this MATE transporter is additionally coupled to protons. How H^+ and Na^+ binding are coupled mechanistically to enable drug antiport is not well understood. In this study, we use molecular dynamics simulations to illuminate the sequence of ion binding event that enable efflux. Understanding this antiport mechanism is important to support the development of novel compounds that specifically inhibit the functional cycle of NorM transporters.

Introduction

Multidrug efflux represents a major problem in healthcare, as it underlies the expulsion of antimicrobal drugs from microbes [1] or drug export from human cells [2] and thus prevents the efficient medication of diseases including bacterial infections and cancer. In bacteria, efflux of drugs is considered to be one of the main drivers for multidrug resistant strains, as reviewed recently [3,4]. Presently, five classes of multidrug efflux pumps have been identified, (a) the ABC (ATP binding cassette) [5], (b) MFS (major facilitator family) [6], (c) RND (resistance nodulation cell division) [7], (d) SMR (small multidrug resistance) [8] and the (e) MATE (multidrug and toxic extrusion) [9] transporters. Multidrug resistance can be caused by all five classes of efflux transporters [10].

MATE transporters are multidrug efflux pumps, which export metabolic waste or a variety of drugs [11] across the cytoplasmic membrane in various organisms such as plants [12], mammals [13] and Gram-negative [14] or Gram-positive [15] bacteria. They are driven by an electrochemical gradient, generated by either Na^+ ions [16], protons [17,18] or a coupled sodium/proton [19] gradient, and are thought to employ an alternative-access mechanism for function. Ion binding to the MATE transporter in the outward facing state induces a large conformational change to the inward facing conformation. Vice versa, drug binding in the inward facing state induces a conformational change from the inward to the outward facing conformation, releasing the drug from the cell. Current spectroscopic data [20], chemical (disulfide) cross-linking experiments [21] and the crystal structures of bacterial sodium [22–24] and proton driven MATE transporters [25,26] have revealed first details of this antiport mechanism. In addition, several recently published crystal structures have been solved in ligand bound states in the outward facing conformation [23,26,27], offering new information on the ligand binding mode of MATE transporters. Further mechanistic information for the proton coupled MATE transporter from *Pyrococcus furiosus* was obtained by using molecular dynamics (MD) and quantum mechanics/molecular mechanics (QM/MM) simulations [28].

Because antimicrobial resistance has evolved into a global health issue, obtaining information on mechanistic features of multidrug efflux pumps, such as MATE transporters, which mediate drug resistance in Gram-positive [29] and Gram-negative bacteria [10], have become essential. In Gram-negative bacteria, such as for example *Vibrio cholera* and *Escherichia coli*, MATE transporters transport drugs across the inner membrane [24]. Understanding these mechanistic features is important for the design of novel inhibitors to prevent drug-extrusion from bacterial cells. All crystallographically resolved bacterial MATE transporters are composed of 12 transmembrane helices. They are divided into two 6 transmembrane helix bundles comprising a two-fold pseudo symmetry, most likely caused by gene duplication [30]. Mammalian MATE transporters have been proposed to harbour a 13^{th} helix [31], which may adjust turnover activities but is not necessary for transport function [32]. In addition, the crystal structures, all determined in the outward facing conformation, show a deep cavity in which the drug is bound before being extruded. The crystal structures of NorM-VC (*Vibrio cholerae*) [22], NorM-NG (*Neisseria gonorrhoeae*) [23] and ClbM (*Escherichia coli*) [24], all resolved in a Rb^+ or Cs^+ bound state, suggest that sodium coupled MATE transporters harbour cation-binding motifs which involve cation-π interactions.

Biochemical data has revealed that mutating a conserved glutamate residue (E251A in the MATE transporter NorM-VP from *Vibrio parahaemolyticus* [33] and E273Q in hMATE1 [18]) causes a loss of transport function. The mutation of homologous residues (E255Q [19] and E261A [23] in

NorM-VC and NorM-NG from *Vibrio cholerae* and *Neisseria gonorrhoeae*, respectively) also affects the function of the protein. It has therefore been concluded that these residues are involved in the transport cycle. In addition, it has been shown recently that alongside the sodium ion, a proton is translocated across the membrane in NorM-VC, potentially by D371 [19]. D371 is located in the vicinity of E255 in NorM-VC [22]. Subsequent to the conformational change to the inward-facing state, the sodium ion and the proton are released into the cytoplasm [19]. Thus, in contrast to other members of the MATE family, the activity of the MATE transporter NorM-VC from *Vibrio cholerae* is coupled to the translocation of two ions (Na^+ and H^+) across the membrane. However, the sequence of ion binding and the structural basis for this unusual two-ion coupling event in this MATE antiporter remain unclear.

To illuminate the sequence of ion binding events which drive drug efflux in NorM-VC, we applied MD simulations, thermodynamic integration (TI) and potential-of-mean-force (PMF) calculations in the outward facing conformation. Understanding the order of events that drive the efflux mechanism of MATE transporters may enable the development of therapeutics that specifically target functionally important transporter states in this cycle and thereby inhibit the extrusion of antibiotics from the bacterial cell.

Methods

System preparation

pK_a values for all titratable groups of the MATE transporter NorM-VC (PDB-ID: 3MKU) [22] were initially calculated by using the H++ webserver [34]. D371 was assumed to be protonated according to previously published experimental results [19]. The pK_a values of E255 and D371 were later recalculated using TI (see below). The Rb^+ ion determined in the crystal structure was exchanged by a physiological Na^+ ion. The MATE transporter was aligned to a POPC bilayer using the program LAMBADA [35], and inserted into the membrane using the g_membed [36,37] module implemented in GROMACS [38]. A concentration of 250 mM NaCl and additional counter ions to neutralize the system were added.

MD simulations

All MD simulations were carried out with the simulation suite GROMACS [38]. We applied the amber_ildn force field for amino acids [39,40], the Berger lipid parameter set [41] for the POPC bilayer and ion parameters developed by Joung et al. [42]. The SPCE water model [43] was used. Pressure and temperature were kept constant at 1 bar and 298 K, using the Parrinello-Rahman barostat [44] and the v-rescale thermostat [45], with coupling constants of 2 ps and 0.5 ps, respectively. Van der Waals interactions were computed with a cut-off of 12 Å. Long range electrostatic interactions were calculated using the Particle Mesh Ewald (PME) method, applying a real space cut-off of 12 Å. We constrained all bonds by applying the LINCS [46] algorithm. The use of the virtual site approach [47] allowed us to employ an integration time-step of 4 fs. This approach attaches a virtual site to non-polar hydrogen atoms, inhibiting their fast bond vibrations which are irrelevant for the conformation of the protein. Periodic boundary conditions were applied in all three directions. An equilibration with sequentially decreased backbone restraints was carried out before starting the production runs.

Free energy calculations – Thermodynamic Integration (TI)

We calculated the pK_a of E255 and D371 in the Na^+ bound state with the Thermodynamic Integration (TI) method, using 32 discrete λ points (0, 0.05, 0.1, 0.15, 0.2, 0.25, 0.3, 0.35, 0.4, 0.45, 0.5, 0.54, 0.58, 0.62, 0.66, 0.7, 0.73, 0.76, 0.79, 0.82, 0.85, 0.87, 0.89, 0.91, 0.93, 0.95, 0.96, 0.97, 0.98, 0.99, 0.995 and 1), and changing all interactions simultaneously. Each window was simulated for 10 ns. To benchmark the pK_a calculations, deprotonation calculations were first carried out in solution for N-acetyl-N'-methyl-L-aspartylamide (AMA), the pK_a value of which has been shown to be 4.08 [48]. These simulations were followed by deprotonation simulations of E255 and D371 in the Na^+ bound and unbound state. All TI simulations were repeated three times. The free energy difference was calculated with the g_bar module as implemented in GROMACS, using the BAR method. A correction as discussed previously [49] was applied; the dielectric constant ε_1 was set to 2 to take the polarisability of the membrane into account, which cannot be represented by a classical force field.

Free energy differences were obtained from the thermodynamic cycle:

Figure 1: Thermodynamic cycle to calculate the change of the deprotonation free energy of a titratable residue inside a protein with respect to a free amino acid in solution.

ΔΔG can now be calculated by ΔΔG=ΔG3-ΔG1 [50] and the pK_a shift (ΔpK_a) can be calculated via [50,51]:

$$\otimes pK_a = pK_a\left(ASP^{protein}\right) - pK_a\left(ASP^{solution}\right) = \frac{1}{2.3\ kT}(\Delta G3\text{-}\Delta G1) = \frac{1}{2.3\ kT}$$

calculations) were performed on a local CPU/GPU cluster at the School of Life Sciences, University of Dundee, and overall entailed a computational cost of ~ 13.300 TFlops.

Results

The Na^+ binding site of NorM-VC

The crystal structure of NorM-VC (pdb-ID: 3MKU) [22] has provided first structural insights into Na^+ binding to MATE transporters and Na^+ translocation, as initially studied biochemically for NorM-VP from *Vibrio parahaemolyticus* [16]. However, the ion binding motif observed in the crystal structure is unusual, as the Rb^+/Cs^+ ion (replacing Na^+) is coordinated by several cation-π interactions to F259 and F429 and an electrostatic interaction with Y367:OH [22]. In contrast, negatively charged residues, namely E255 and D371, which have been shown to be functionally important in homologous proteins [23,33], are only found in the distant vicinity of the ion. The overall structure and a close-up view of the ion binding site are shown in Figure 2a.

Molecular dynamics (MD) simulations of NorM-VC have indeed suggested that the Na^+ ion is coordinated by E255 and D371 [53,54]. In these previous simulations, both carboxylate groups were assumed to be in the charged state. However, this assumption seems to be inconsistent with recently released experimental data, which demonstrated that, in addition to Na^+, a proton is translocated across the membrane [19]. The likely key residue for coupled proton transport was identified as D371 [19]. To obtain further insights into the ion binding site and the coupling between Na^+ and proton binding, we therefore first performed MD simulations, in which D371 was modelled as protonated, in accordance with the interpretation of the earlier experimental findings.

We set up six replicas under three different simulation conditions. In the first set, free simulations of NorM-VC in a model membrane were carried out. In the second set, we used a restraint potential (10 kJ/(mol*nm^2)) on all protein backbone atoms in order to inhibit large-scale conformational changes of the protein. In addition, we simulated NorM-VC without restraints but under application of an electric field (~400 mV) in the third set to mimic the microbial membrane potential. The membrane potential in bacteria has been measured at ~ -140 mV for *Escherichia coli* [55]. In the biochemical experiments, which demonstrated proton translocation through NorM-VC, a membrane potential of ~ -160 mV was applied [19]. Usually, simulation studies of membrane proteins – with the exception of ion channels – are conducted without taking the membrane voltage into account. However, the membrane electric field, especially in microbes, can be anticipated to exert a considerable influence on the conformational ensemble of membrane proteins and ion binding events [56]. We used a slightly raised voltage here in order to accelerate molecular motions on the computationally accessible simulation timescale. The voltage we used, however, is at the lower end of the range commonly applied for similar studies of membrane proteins in simulations, for example for ion channels [57,58].

In the equilibrium simulations, we observe stable ion binding near the crystallographically determined site only when backbone restraints are applied, while in free simulations without restraints the binding stability of the ion is markedly diminished (Figure S1). By contrast, simulations in which we apply an electric field across the membrane result in stable binding of the Na^+ ion in the experimentally reported binding region and well-defined close interactions between the ion and the protein (Figure 2b). Figure 2c shows a representative binding

configuration, in which the Na^+ ion exhibits interactions with E255:Oεx, D371:Oδ1, Q374:Oε1 and a water molecule. The binding site is further stabilized by a hydrogen bond between Y398:OH and E255:Oεx. A similar interaction has been found in a Na^+ binding site of a membrane embedded rotor protein [59], where a mutation of Tyr to Phe, abolishing the hydrogen bond between Y:OH – E:Oεx, led to an altered ion (Na^+ vs. H^+) selectivity [60,61].

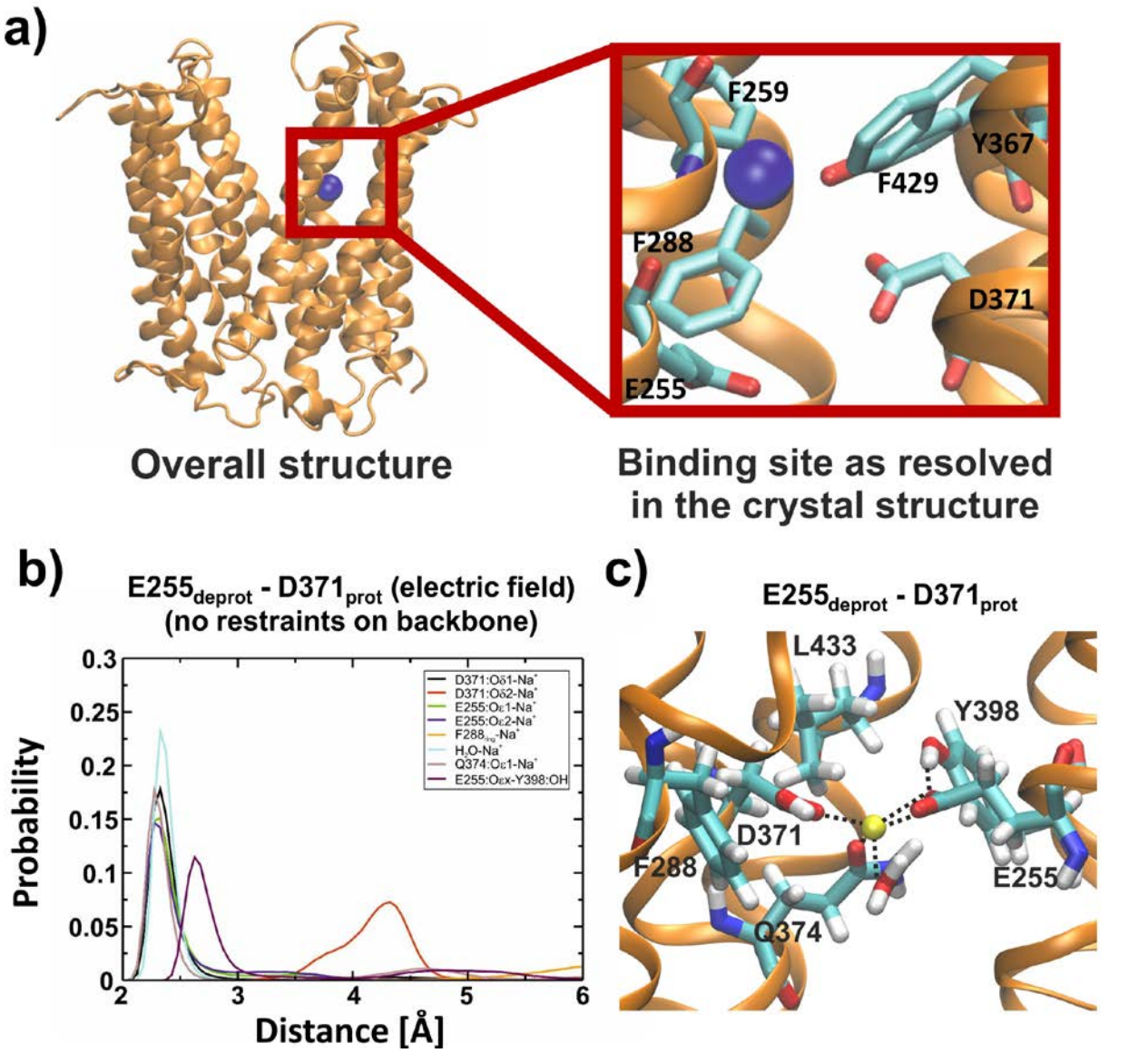

Figure 2: (a) Overall structure of the MATE transporter NorM-VC (left; PDB-ID: 3MKU) and close-up view of the ion binding site (right), as resolved by X-ray crystallography. All figures containing molecular information were generated using VMD [62]. (b) Probability distribution of specific molecular interactions within the binding site. (c) Representative snapshot of the ion binding configuration observed in our simulations under membrane voltage.

Protonation state of the ion binding site

Next, we were interested in determining the protonation state of the binding site in more detail. Protonation changes of ionisable residues require either the presence of neighbouring residues, which can accept or donate protons from/to the ionisable group, or an aqueous environment. Because no ionisable residues are located within a distance of 5 Å from E255:Oεx or D371:Oδx, we analysed the hydration profile of this protein region after 100 ns of MD equilibration in three simulation setups with the program trj_cavity [63], probing all possible combinations of E255 and D371 protonation states ($E255_{deprot}/D371_{prot}$, $E255_{prot}/D371_{deprot}$, $E255_{deprot}/D371_{deprot}$). The doubly protonated state ($E255_{prot}/D371_{prot}$) was not further studied because previous simulations of NorM-VC in the analogous state did not show any sodium ion binding to the homologous residues (E261 and D377) [64]. The result for each state is displayed in Figure 3. As can be seen, both E255 and D371 are fully hydrated in all protonation states. We therefore conclude that protonation events can occur directly between water and either residue. We ascribe the high hydration level observed in all simulations to the presence of at least one charged carboxylate group, which has previously been reported to increase the local hydration level in different proteins [65,66]. In addition, continuous solvation allows the ion to enter the binding site from the bulk solution in all possible protonation states of E255 and D371 (see Figure 5, below).

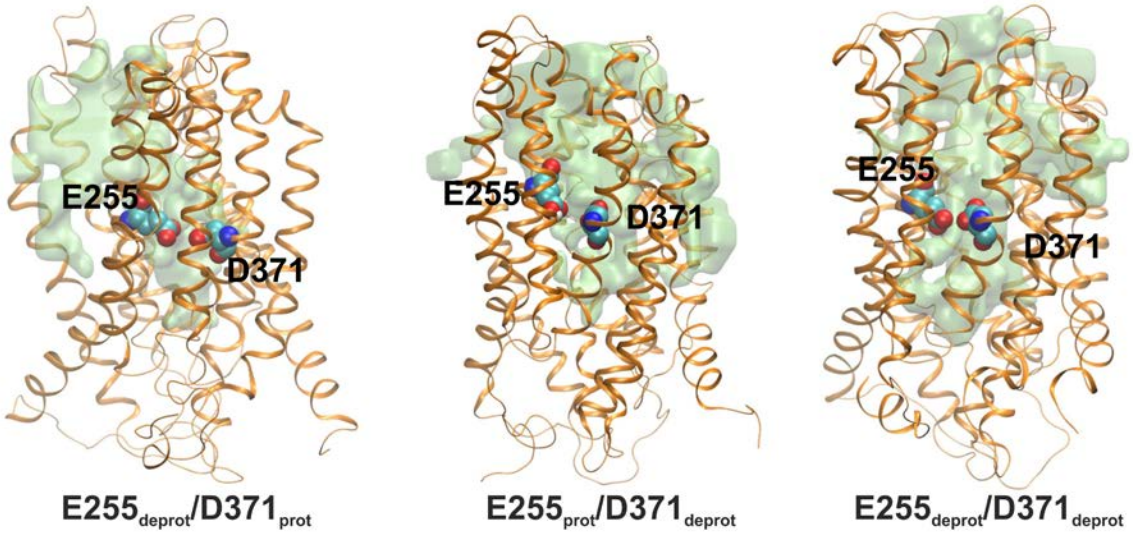

Figure 3: Hydration profile of the simulated systems with different protonation states. The solvation profile is shown in transparent light green and E255 and D377 are displayed as van der Waals spheres.

To further investigate the protonation state of the ion binding region, and how protonation of this site might depend on the presence of the Na^+ ion, we carried out TI calculations to determine the pK_a values of E255 and D371 with and without bound ion. We calculated the free energy necessary to deprotonate the respective protein side chains (ΔG_{deprot}) and used the ionisation free energy and pK_a of N-acetyl-N'-methyl-L-aspartylamide (AMA) as reference, a compound commonly used as benchmark for amino acid residues carrying carboxylate groups.

Our results show a $\Delta\Delta G_{deprot}$ for D371 with respect to AMA of 26.9 +/- 4.8 kcal/mol in the Na^+-bound state, and of 32.5 +/- 4.0 kcal/mol in the Na^+-unbound state, when E255 is charged. In turn, when D371 is assumed to be charged, we obtain a deprotonation penalty for E255 relative to AMA of 18.2 +/- 4.0 kcal/mol in the Na^+ bound state, and of 22.9 +/- 0.6 kcal/mol in the Na^+ unbound state. These values correspond to an upward pK_a shift of 13.4 and 16.9 units for the deprotonation of E255 in the presence or absence of Na^+, respectively. Similarly, the pK_a of D371 is shifted upwards by 19.8 and 23.9 units in Na^+-bound and -unbound conditions, respectively (Figure 4). pK_a shifts of comparable magnitude have previously been observed in the closed conformation of a F-type ATP synthase rotor ring [67].

These results show that at least one proton is continuously bound to one of the carboxylate residues (E255 or D371) in the drug-free state, irrespective of the presence or absence of a bound Na^+ ion. In addition, our pK_a calculations show that amongst the two scenarios, deprotonation of D371 incurs a substantially higher free energy penalty than deprotonation of E255, and therefore we conclude that, out of this dyad of ionisable side chains, D371 is more likely to carry the proton. This result is in good agreement with a previous study on a molecular rotor, where two carboxylate groups bind to a sodium ion during the Na^+ translocation mechanism, but one carboxylate group is protonated at any time (Na^+ bound or unbound) under physiological conditions [68]. Our finding is also in agreement with the observation that the E255Q mutant has been shown to markedly decrease transport activity in intact cells (NorM-VC) [19].

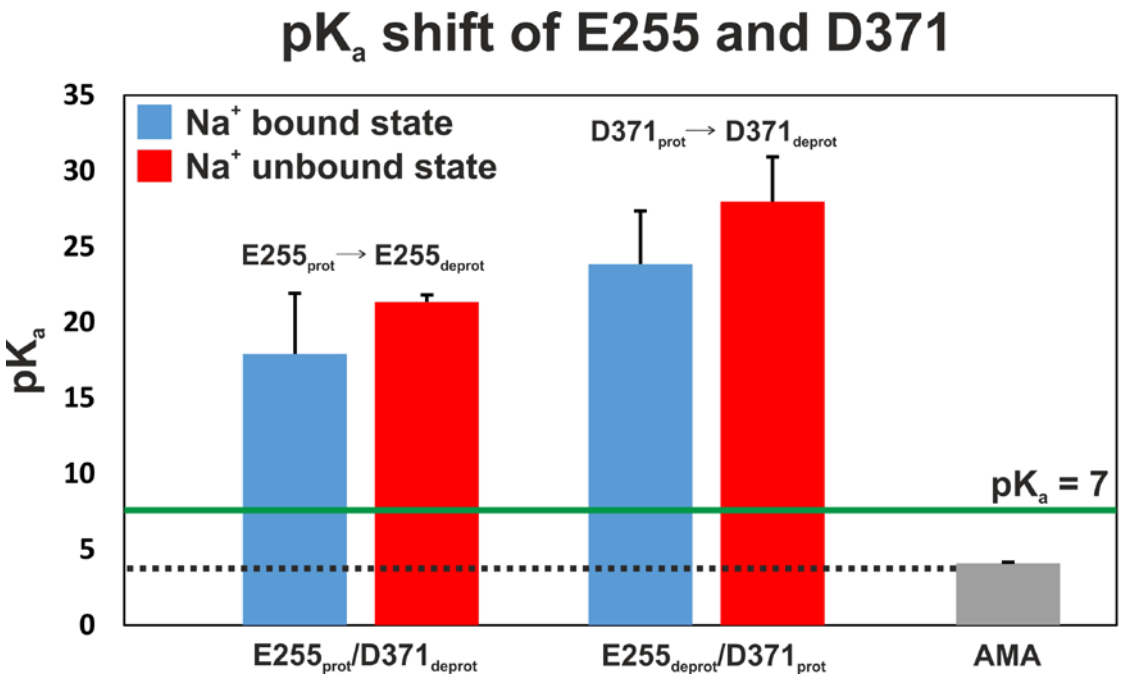

Figure 4: pK_a shifts of E255 and D371 relative to the benchmark compound AMA (grey). Results for the Na^+ bound state are shown in blue, results for the ion unbound state are shown in red. The deprotonation reactions $E255_{prot}$ $E255_{deprot}$ and $D371_{prot}$ $D371_{deprot}$ were investigated, while the remaining ionisable side chain in the dyad was kept charged in either case.

The predicted K_d for Na^+ binding is in good agreement with experimental data

Having established the most likely protonation states of the Na^+ binding region, we conducted potential of mean force calculations in order to evaluate if these states reproduce experimental binding energetics for the Na^+ ion. Our umbrella sampling calculations show that in cases, in which one of the ionisable residues forming the Na^+ binding site is protonated, similar free energies of binding the Na^+ ion from the bulk solution of ~6.1 +/- 1.0 kcal/mol and ~5.0 +/- 0.5 kcal/mol are obtained for $E255_{deprot}/D371_{deprot}$ (Fig. 5 - black) and $E255_{prot}/D371_{prot}$ (Fig.5 - red), respectively. The standard deviation in the PMFs is comparable to errors reported before, for instance for ion movement in the δ-opioid and M2 muscarinic G-protein coupled receptors, where a standard deviation of 0.6 kcal/mol is observed [69]. The affinity of NorM-VC for Na^+ arises mainly from local interactions near the ion binding site, and therefore the overall binding free energies are well-defined, despite the occurrence of fluctuations in the PMF within the wide entrance vestibule of NorM. Due to the absence of structural data of the inward-facing conformation of NorM-VC, both calculations were carried out for the outward-facing conformation of NorM-VC.

The value we obtained for both scenarios is in good agreement with the measured binding free energy of 5.6 kcal/mol (corresponding to a K_D of 73 μM) [19]. Experimental data has additionally shown, however, that the ion binding affinity is not greatly affected by the D371N mutation (K_D = 90 μM) [19], indicating again that in the wild type D371 is protonated in the outward-facing conformation (see section above).

We also calculated the PMF for the $E255_{prot}/D371_{deprot}$ state. This results in a free energy difference of 11.2 +/- 1.0 kcal/mol (Figure S2), which exceeds the available experimental data by a factor of ~2. Further, our TI calculations do not support a doubly charged Na^+ binding site, neither in the presence nor absence of a Na^+ ion. Thus, we conclude that the basis for Na^+/H^+ coupling in the MATE transporter NorM is an ion binding site composed of a negatively charged $E255_{deprot}$ and a protonated $D371_{prot}$ side chain, which sustains its protonated state, even after Na^+ binding has taken place.

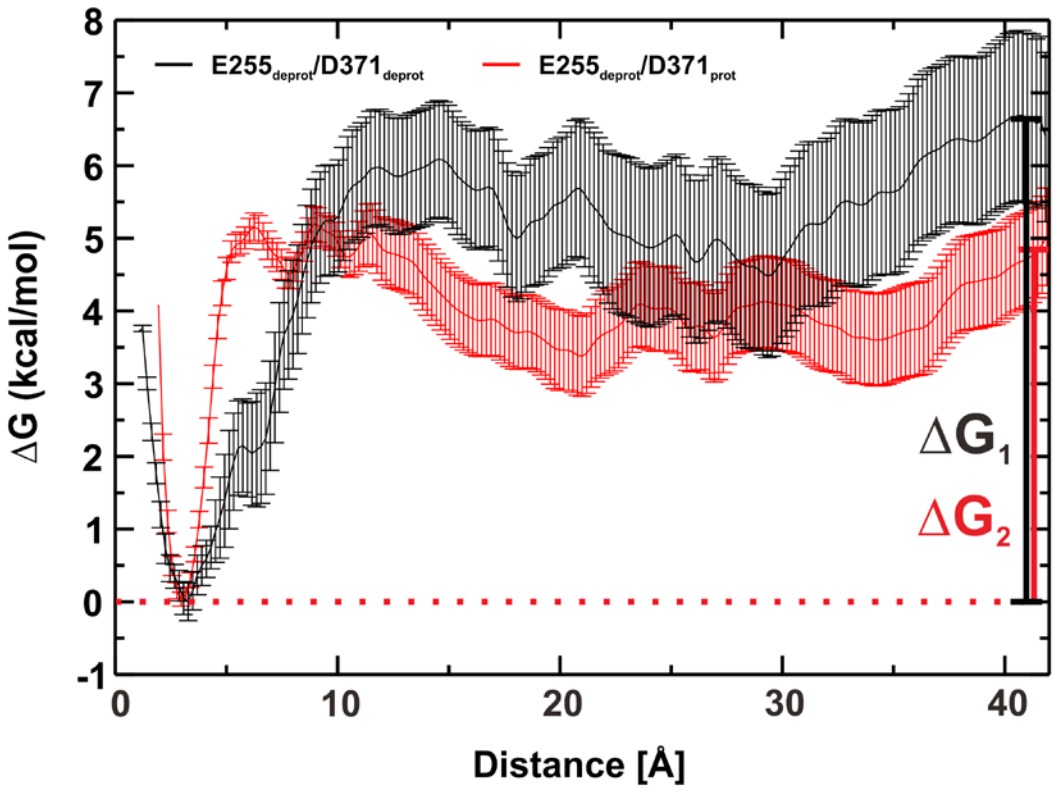

Figure 5: Potential of Mean Force (PMF) of Na^+ ion translocation from the binding site to the bulk in the NorM-VC $E255_{deprot}/D371_{deprot}$ (black) and $E255_{deprot}/D371_{prot}$ (red) states.

Discussion

Bacteria have evolved a variety of ways to protect themselves from external noxious compounds. For example, they can control the inward permeation of compounds across specialised proteins [70,71], and they are able to modify chemical compounds [72] and mutate internal proteins [73] to prevent antibiotics binding to a target. Furthermore, bacteria can form impermeable layers around bacterial communities (biofilms) [74,75], and they are capable of efficiently extruding a wide range of toxic compounds by efflux transporters [10].

MATE transporters are multidrug efflux proteins which contribute to the emergence of multidrug resistance in bacteria. Previous studies have suggested that the NorM family transports Na^+ and drugs via an antiport mechanism [16]. However, recent experimental data have shown that NorM-VC is coupled to both Na^+ and H^+ [19] to optimally induce the conformational change from the outward to the inward facing conformation. The same ion-coupling behavior has recently been observed for the MATE transporter ClbM from *Escherichia coli* [76]. The order of ion binding in the outward facing conformation and the order of ion release in the inward facing conformation have however remained unclear.

Our molecular dynamics simulations suggest that sodium binding occurs near the site defined in the crystal structure of NorM-VC, but that it involves interactions that differ from those proposed in the crystal structure. Some of the detailed interactions we observe may be influenced by the presence of the strong membrane voltage in microbes, which attracts positively charged ions towards the intracellular side. Our MD simulations show that the sodium ion is stably bound to its

binding site when applying an electric field, but not when the electric field is turned off (Figure 2, S1).

Furthermore, we modelled D371 as protonated in our initial simulations, following indications from experimental data [19]. To further investigate if at least one of the carboxylate residues is protonated at any time in the outward facing conformation of NorM-VC, we calculated the pK_a of the two ionisable residues forming the Na^+ binding site, both in the presence and absence of a Na^+ ion in the binding site. It should be noted that the drug was absent during our simulations because it has not been resolved in any NorM-VC crystal structure so far.

According to our results, one of the carboxylate groups is always protonated in the outward facing conformation, regardless of the presence of the Na^+ ion. Previously, it has been assumed that both E255 and D371 are deprotonated [53,54]. Our calculations indicate that D371 is more likely to be protonated than E255 in this conformation. The presence of a positively charged drug may alter this behavior, however it is likely that E255 would have a reduced propensity to be protonated in that case, as the positive charge of the drug can be expected to reside in the vicinity of this residue. Thus we suggest that the proton is more likely to be directly transferred to D371 from the bulk solution and not via E255. It is important to note that polarization and charge-transfer effects, which are not included in common classical force-field models, are expected to have an influence on ion binding and the binding free energy of ions to proteins. However, a recent study revealed that classical force-field studies, such as the one presented here, offer a reasonably good description of these molecular interactions and the corresponding energies in the case of monovalent ions such as Na^+ [77].

Taken together, our results suggest a model for the order of ion binding in the outward facing conformation, with important mechanistic implications for the mode of operation of the NorM-VC MATE transporter. We propose that, as a first step, a proton binds to D371, after the conformational change from the inward- to the outward facing conformation has occurred (Figure 6). Protonation of D371 is then followed by Na^+ binding. The ion travels inward via a hydrated funnel in the vestibule of the protein, which connects the bulk and the ion binding site. Na^+ binding subsequently releases the bound drug from the protein [23,64]. In the drug-free state, a conformational change from the outward to the inward facing conformation is induced, from which the ions are released to the intracellular side, and which takes up a new drug molecule. This conformational change is driven by the ion and voltage gradients across the membrane, which attract Na^+ and H^+ ions into the cytoplasm. We speculate that D371 is either well solvated or other titratable residues reside nearby in that conformation, such that under physiological conditions its side chain becomes deprotonated there. This change of the protonation state may also be required to bind the positively charged drug. The order and details of the intracellular events, however, remain unclear, owing to the lack of structural data of the inward facing state.

Additional biochemical, structural and computational studies are necessary to elucidate the mechanistic features of the transport mechanism of NorM-VC, and to address the question if the Na^+/H^+ antiport mechanism present in NorM-VC from *Vibrio cholerae* [19] can be transferred to other NorM or other MATE transporters. Dual ion coupling has, for instance, recently been shown to occur in ClbM from *Escherichia coli* [76]. However, there may be crucial mechanistic differences in the ion coupling behavior of several NorM transporters (coupling to H^+ instead to Na^+), as previously proposed for NorM-PS from *Pseudomonas stutzeri* based on biochemical data [78]. The reasons for the different ion selectivity and the mechanistic diversity in the NorM family need to be clarified by further studies.

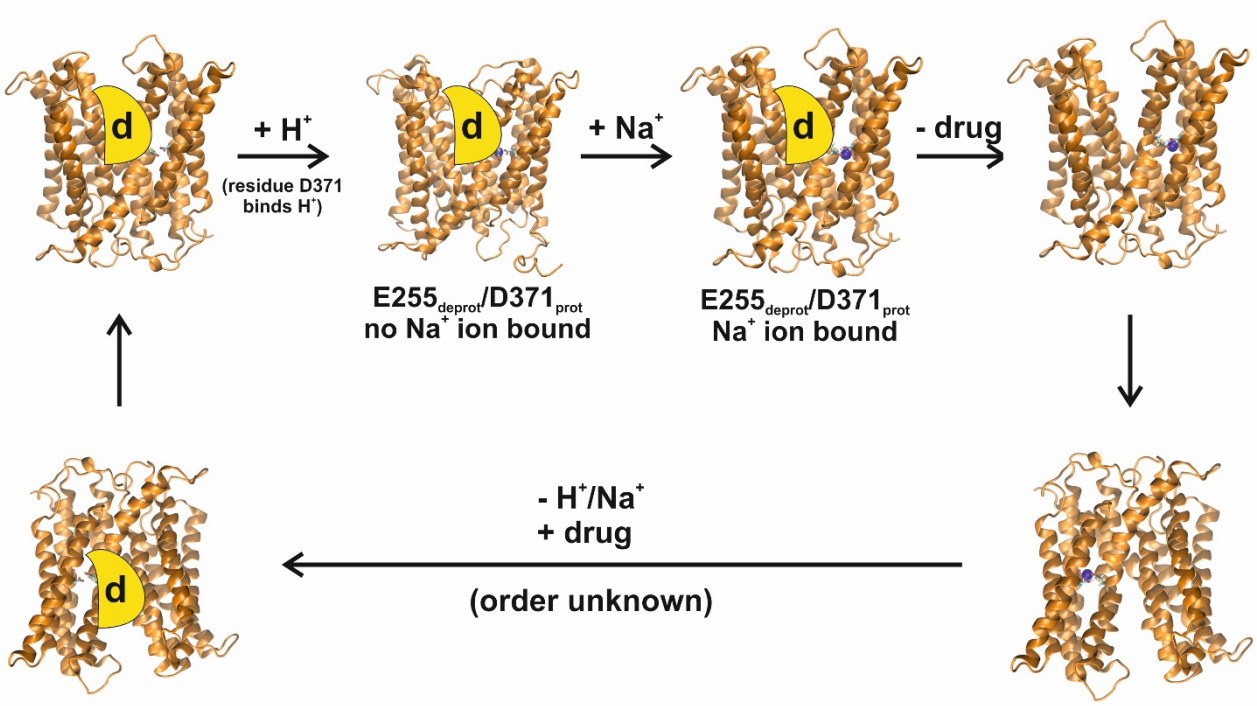

Figure 6: Proposed mechanism of ion/drug coupling of the MATE transporter NorM-VC from *Vibrio cholerae*. After the conformational change from the inward to the outward facing conformation (left) has taken place, a proton binds to D371, followed by Na^+ binding. Following these events, the drug is released and the conformational change from the outward to the inward facing conformation is induced, which allows the protein to release the ions (H^+ and Na^+) towards the cytoplams and to bind a new drug molecule. The order of the cytoplasmic events is still unknown however, to the lack of structural data.

To summarise, drug efflux in bacteria, a strong contributor to antimicrobial resistance, is one of the major problems in the development of new antibiotics. In this study we suggest how the first step of coupled proton-ion transport may occur in the MATE transporter NorM-VC from *Vibrio cholerae*, a protein that efficiently expels antibiotics from bacterial cells. This additional insight on the ion translocation mechanism may aid the design of specifically targeted drugs inhibiting the export of antibiotics.

Acknowledgements

This work was funded by SUPA (Scottish University Physics Alliance).

References

[1] S. Kumar, M.F. Varela, Biochemistry of Bacterial Multidrug Efflux Pumps, Int. J. Mol. Sci. 13 (2012) 4484–4495. doi:10.3390/ijms13044484.

[2] K.M. Pluchino, M.D. Hall, A.S. Goldsborough, R. Callaghan, M.M. Gottesman, Collateral sensitivity as a strategy against cancer multidrug resistance, Drug Resist. Updat. 15 (2012) 98–105. doi:10.1016/j.drup.2012.03.002.

[3] H. Nikaido, J.-M. Pagès, Broad-specificity efflux pumps and their role in multidrug resistance of Gram-negative bacteria, FEMS Microbiol. Rev. 36 (2012) 340–363. doi:10.1111/j.1574-6976.2011.00290.x.

[4] D. Du, H.W. van Veen, B.F. Luisi, Assembly and operation of bacterial tripartite multidrug efflux pumps, Trends Microbiol. 23 (2015) 311–319. doi:10.1016/j.tim.2015.01.010.

[5] J. Lubelski, W.N. Konings, A.J.M. Driessen, Distribution and Physiology of ABC-Type Transporters Contributing to Multidrug Resistance in Bacteria, Microbiol. Mol. Biol. Rev. 71 (2007) 463–476. doi:10.1128/MMBR.00001-07.

[6] M.H. Saier, J.T. Beatty, A. Goffeau, K.T. Harley, W.H. Heijne, S.-C.C. Huang, D.L. Jack, P.S. Jähn, K. Lew, J. Liu, S.S. Pao, I.T. Paulsen, T.T. Tseng, P.S. Virk, The major facilitator superfamily., J. Mol. Microbiol. Biotechnol. 1 (1999) 257–79. http://www.horizonpress.com/backlist/jmmb/v/v1/v1n2/09.pdf.

[7] T.T. Tseng, K.S. Gratwick, J. Kollman, D. Park, D.H. Nies, A. Goffeau, M.H. Saier, The RND permease superfamily: an ancient, ubiquitous and diverse family that includes human disease and development proteins., J. Mol. Microbiol. Biotechnol. 1 (1999) 107–25. http://www.ncbi.nlm.nih.gov/pubmed/10941792.

[8] D.C. Bay, K.L. Rommens, R.J. Turner, Small multidrug resistance proteins: a multidrug transporter family that continues to grow., Biochim. Biophys. Acta. 1778 (2008) 1814–38. doi:10.1016/j.bbamem.2007.08.015.

[9] M.H. Brown, I.T. Paulsen, R.A. Skurray, The multidrug efflux protein NorM is a prototype of a new family of transporters, Mol. Microbiol. 31 (1999) 394–395. doi:10.1046/j.1365-2958.1999.01162.x.

[10] D. Du, H.W. van Veen, S. Murakami, K.M. Pos, B.F. Luisi, Structure, mechanism and cooperation of bacterial multidrug transporters, Curr. Opin. Struct. Biol. 33 (2015) 76–91. doi:10.1016/j.sbi.2015.07.015.

[11] A. Begum, M.M. Rahman, W. Ogawa, T. Mizushima, T. Kuroda, T. Tsuchiya, Gene Cloning and Characterization of Four MATE Family Multidrug Efflux Pumps from Vibrio cholerae Non-O1, Microbiol. Immunol. 49 (2005) 949–957. doi:10.1111/j.1348-0421.2005.tb03690.x.

[12] J. V Magalhaes, J. Liu, C.T. Guimarães, U.G.P. Lana, V.M.C. Alves, Y.-H. Wang, R.E. Schaffert, O.A. Hoekenga, M.A. Piñeros, J.E. Shaff, P.E. Klein, N.P. Carneiro, C.M. Coelho, H.N. Trick, L. V Kochian, A gene in the multidrug and toxic compound extrusion (MATE) family confers aluminum tolerance in sorghum, Nat. Genet. 39 (2007) 1156–1161. doi:10.1038/ng2074.

[13] S. Masuda, T. Terada, A. Yonezawa, Y. Tanihara, K. Kishimoto, T. Katsura, O. Ogawa, K. Inui, Identification and functional characterization of a new human kidney-specific H+/organic cation antiporter, kidney-specific multidrug and toxin extrusion 2., J. Am. Soc.

Nephrol. 17 (2006) 2127–35. doi:10.1681/ASN.2006030205.

[14] Y. Morita, K. Kodama, S. Shiota, T. Mine, A. Kataoka, T. Mizushima, T. Tsuchiya, NorM, a putative multidrug efflux protein, of Vibrio parahaemolyticus and its homolog in Escherichia coli., Antimicrob. Agents Chemother. 42 (1998) 1778–82. http://www.ncbi.nlm.nih.gov/pubmed/9661020.

[15] G.W. Kaatz, F. McAleese, S.M. Seo, Multidrug Resistance in Staphylococcus aureus Due to Overexpression of a Novel Multidrug and Toxin Extrusion (MATE) Transport Protein, Antimicrob. Agents Chemother. 49 (2005) 1857–1864. doi:10.1128/AAC.49.5.1857-1864.2005.

[16] Y. Morita, A. Kataoka, S. Shiota, T. Mizushima, T. Tsuchiya, NorM of Vibrio parahaemolyticus Is an Na+-Driven Multidrug Efflux Pump, J. Bacteriol. 182 (2000) 6694–6697. doi:10.1128/JB.182.23.6694-6697.2000.

[17] G.-X. He, T. Kuroda, T. Mima, Y. Morita, T. Mizushima, T. Tsuchiya, An H+-Coupled Multidrug Efflux Pump, PmpM, a Member of the MATE Family of Transporters, from Pseudomonas aeruginosa, J. Bacteriol. 186 (2004) 262–265. doi:10.1128/JB.186.1.262-265.2004.

[18] M. Otsuka, T. Matsumoto, R. Morimoto, S. Arioka, H. Omote, Y. Moriyama, A human transporter protein that mediates the final excretion step for toxic organic cations, Proc. Natl. Acad. Sci. 102 (2005) 17923–17928. doi:10.1073/pnas.0506483102.

[19] Y. Jin, A. Nair, H.W. van Veen, Multidrug Transport Protein NorM from Vibrio cholerae Simultaneously Couples to Sodium- and Proton-Motive Force, J. Biol. Chem. 289 (2014) 14624–14632. doi:10.1074/jbc.M113.546770.

[20] P.R. Steed, R.A. Stein, S. Mishra, M.C. Goodman, H.S. McHaourab, Na^+-substrate coupling in the multidrug antiporter norm probed with a spin-labeled substrate., Biochemistry. 52 (2013) 5790–9. doi:10.1021/bi4008935.

[21] M. Radchenko, R. Nie, M. Lu, Disulfide Cross-linking of a Multidrug and Toxic Compound Extrusion Transporter Impacts Multidrug Efflux, J. Biol. Chem. 291 (2016) 9818–9826. doi:10.1074/jbc.M116.715227.

[22] X. He, P. Szewczyk, A. Karyakin, M. Evin, W.-X. Hong, Q. Zhang, G. Chang, Structure of a cation-bound multidrug and toxic compound extrusion transporter, Nature. 467 (2010) 991–994. doi:10.1038/nature09408.

[23] M. Lu, J. Symersky, M. Radchenko, A. Koide, Y. Guo, R. Nie, S. Koide, Structures of a Na+-coupled, substrate-bound MATE multidrug transporter, Proc. Natl. Acad. Sci. 110 (2013) 2099–2104. doi:10.1073/pnas.1219901110.

[24] J.J. Mousa, Y. Yang, S. Tomkovich, A. Shima, R.C. Newsome, P. Tripathi, E. Oswald, S.D. Bruner, C. Jobin, MATE transport of the E. coli-derived genotoxin colibactin, Nat. Microbiol. 1 (2016) 15009. doi:10.1038/nmicrobiol.2015.9.

[25] Y. Tanaka, C.J. Hipolito, A.D. Maturana, K. Ito, T. Kuroda, T. Higuchi, T. Katoh, H.E. Kato, M. Hattori, K. Kumazaki, T. Tsukazaki, R. Ishitani, H. Suga, O. Nureki, Structural basis for the drug extrusion mechanism by a MATE multidrug transporter, Nature. 496

(2013) 247–251. doi:10.1038/nature12014.

[26] M. Lu, M. Radchenko, J. Symersky, R. Nie, Y. Guo, Structural insights into H+-coupled multidrug extrusion by a MATE transporter, Nat. Struct. Mol. Biol. 20 (2013) 1310–1317. doi:10.1038/nsmb.2687.

[27] M. Radchenko, J. Symersky, R. Nie, M. Lu, Structural basis for the blockade of MATE multidrug efflux pumps, Nat. Commun. 6 (2015) 7995. doi:10.1038/ncomms8995.

[28] W. Nishima, W. Mizukami, Y. Tanaka, R. Ishitani, O. Nureki, Y. Sugita, Mechanisms for Two-Step Proton Transfer Reactions in the Outward-Facing Form of MATE Transporter, Biophys. J. 110 (2016) 1346–1354. doi:10.1016/j.bpj.2016.01.027.

[29] B.D. Schindler, G.W. Kaatz, Multidrug efflux pumps of Gram-positive bacteria, Drug Resist. Updat. 27 (2016) 1–13. doi:10.1016/j.drup.2016.04.003.

[30] H. Omote, M. Hiasa, T. Matsumoto, M. Otsuka, Y. Moriyama, The MATE proteins as fundamental transporters of metabolic and xenobiotic organic cations, Trends Pharmacol. Sci. 27 (2006) 587–593. doi:10.1016/j.tips.2006.09.001.

[31] X. Zhang, S.H. Wright, MATE1 has an external COOH terminus, consistent with a 13-helix topology., Am. J. Physiol. Renal Physiol. 297 (2009) F263-71. doi:10.1152/ajprenal.00123.2009.

[32] X. Zhang, X. He, J. Baker, F. Tama, G. Chang, S.H. Wright, Twelve Transmembrane Helices Form the Functional Core of Mammalian MATE1 (Multidrug and Toxin Extruder 1) Protein, J. Biol. Chem. 287 (2012) 27971–27982. doi:10.1074/jbc.M112.386979.

[33] M. Otsuka, M. Yasuda, Y. Morita, C. Otsuka, T. Tsuchiya, H. Omote, Y. Moriyama, Identification of Essential Amino Acid Residues of the NorM Na+/Multidrug Antiporter in Vibrio parahaemolyticus, J. Bacteriol. 187 (2005) 1552–1558. doi:10.1128/JB.187.5.1552-1558.2005.

[34] R. Anandakrishnan, B. Aguilar, A. V. Onufriev, H++ 3.0: automating pK prediction and the preparation of biomolecular structures for atomistic molecular modeling and simulations, Nucleic Acids Res. 40 (2012) W537–W541. doi:10.1093/nar/gks375.

[35] T.H. Schmidt, C. Kandt, LAMBADA and InflateGRO2: Efficient Membrane Alignment and Insertion of Membrane Proteins for Molecular Dynamics Simulations, J. Chem. Inf. Model. 52 (2012) 2657–2669. doi:10.1021/ci3000453.

[36] S.O. Yesylevskyy, ProtSqueeze: simple and effective automated tool for setting up membrane protein simulations., J. Chem. Inf. Model. 47 (2007) 1986–94. doi:10.1021/ci600553y.

[37] M.G. Wolf, M. Hoefling, C. Aponte-Santamaría, H. Grubmüller, G. Groenhof, g_membed: Efficient insertion of a membrane protein into an equilibrated lipid bilayer with minimal perturbation, J. Comput. Chem. 31 (2010) 2169–2174. doi:10.1002/jcc.21507.

[38] S. Pronk, S. Pall, R. Schulz, P. Larsson, P. Bjelkmar, R. Apostolov, M.R. Shirts, J.C. Smith, P.M. Kasson, D. van der Spoel, B. Hess, E. Lindahl, GROMACS 4.5: a high-throughput and highly parallel open source molecular simulation toolkit, Bioinformatics. 29 (2013) 845–854. doi:10.1093/bioinformatics/btt055.

[39] V. Hornak, R. Abel, A. Okur, B. Strockbine, A. Roitberg, C. Simmerling, Comparison of multiple Amber force fields and development of improved protein backbone parameters, Proteins Struct. Funct. Bioinforma. 65 (2006) 712–725. doi:10.1002/prot.21123.

[40] K. Lindorff-Larsen, S. Piana, K. Palmo, P. Maragakis, J.L. Klepeis, R.O. Dror, D.E. Shaw, Improved side-chain torsion potentials for the Amber ff99SB protein force field, Proteins Struct. Funct. Bioinforma. 78 (2010) 1950–1958. doi:10.1002/prot.22711.

[41] O. Berger, O. Edholm, F. Jahnig, Molecular Dynamics Simulations of a Fluid Bilayer of Dipalmitoylphosphatidylcholine at Full Hydration, Constant Pressure, and Constant Temperature, Biophys. J. 72 (1997) 2002–2013. doi:10.1016/S0006-3495(97)78845-3.

[42] I.S. Joung, T.E. Cheatham, Determination of alkali and halide monovalent ion parameters for use in explicitly solvated biomolecular simulations., J. Phys. Chem. B. 112 (2008) 9020–41. doi:10.1021/jp8001614.

[43] H.J.C. Berendsen, J.R. Grigera, T.P. Straatsma, The Missing Term in Effective Pair Potentials, J. Phys. Chem. 91 (1987) 6269–6271. doi:10.1021/j100308a038.

[44] M. Parrinello, A. Rahman, Polymorphic transitions in single crystals: A new molecular dynamics method, J. Appl. Phys. 52 (1981) 7182–7190. doi:10.1063/1.328693.

[45] G. Bussi, D. Donadio, M. Parrinello, Canonical sampling through velocity rescaling, J. Chem. Phys. 126 (2007) 14101. doi:10.1063/1.2408420.

[46] B. Hess, H. Bekker, H.J.C. Berendsen, J.G.E.M. Fraaije, LINCS: A linear constraint solver for molecular simulations, J. Comput. Chem. 18 (1997) 1463–1472. doi:10.1002/(SICI)1096-987X(199709)18:12<1463::AID-JCC4>3.0.CO;2-H.

[47] K.A. Feenstra, B. Hess, H.J.C. Berendsen, Improving e -scale molecular dynamics simulations of hydrogen-rich systems, J. Comput. Chem. 20 (1999) 786—798. doi:10.1002/(SICI)1096-987X(199906)20:8<786::AID-JCC5>3.0.CO;2-B.

[48] Y. Nozaki, C. Tanford, Intrinsic dissociation constants of aspartyl and glutamyl carboxyl groups., J. Biol. Chem. 242 (1967) 4731–5. http://www.ncbi.nlm.nih.gov/pubmed/6061418 (accessed June 29, 2016).

[49] J.S. Hub, B.L. de Groot, H. Grubmüller, G. Groenhof, Quantifying Artifacts in Ewald Simulations of Inhomogeneous Systems with a Net Charge, J. Chem. Theory Comput. 10 (2014) 381–390. doi:10.1021/ct400626b.

[50] M. Saito, Molecular dynamics/free energy study of a protein in solution with all degrees of freedom and long-range Coulomb interactions, J. Phys. Chem. 99 (1995) 17043–17048. doi:10.1021/j100046a033.

[51] W.L. Jorgensen, J.M. Briggs, A priori pKa calculations and the hydration of organic anions, J. Am. Chem. Soc. 111 (1989) 4190–4197. doi:10.1021/ja00194a007.

[52] J.S. Hub, B.L. de Groot, D. van der Spoel, g_wham—A Free Weighted Histogram Analysis Implementation Including Robust Error and Autocorrelation Estimates, J. Chem. Theory Comput. 6 (2010) 3713–3720. doi:10.1021/ct100494z.

[53] S. Vanni, P. Campomanes, M. Marcia, U. Rothlisberger, Ion Binding and Internal

Hydration in the Multidrug Resistance Secondary Active Transporter NorM Investigated by Molecular Dynamics Simulations, Biochemistry. 51 (2012) 1281–1287. doi:10.1021/bi2015184.

[54] J. Song, C. Ji, J.Z.H. Zhang, Insights on Na + binding and conformational dynamics in multidrug and toxic compound extrusion transporter NorM, Proteins Struct. Funct. Bioinforma. 82 (2014) 240–249. doi:10.1002/prot.24368.

[55] H. Felle, J.S. Porter, C.L. Slayman, H.R. Kaback, Quantitative measurements of membrane potential in Escherichia coli, Biochemistry. 19 (1980) 3585–3590. doi:10.1021/bi00556a026.

[56] A.E. Cohen, V. Venkatachalam, Bringing Bioelectricity to Light, Annu. Rev. Biophys. 43 (2014) 211–32. doi:10.1146/annurev-biophys-051013-022717.

[57] M.Ø. Jensen, V. Jogini, M.P. Eastwood, D.E. Shaw, Atomic-level simulation of current–voltage relationships in single-file ion channels, J. Gen. Physiol. 141 (2013) 619–632. doi:10.1085/jgp.201210820.

[58] T. Sumikama, S. Oiki, Digitalized K^+ Occupancy in the Nanocavity Holds and Releases Queues of K^+ in a Channel, J. Am. Chem. Soc. 138 (2016) 10284–10292. doi:10.1021/jacs.6b05270.

[59] T. Meier, A. Krah, P.J. Bond, D. Pogoryelov, K. Diederichs, J.D. Faraldo-Gómez, Complete Ion-Coordination Structure in the Rotor Ring of Na+-Dependent F-ATP Synthases, J. Mol. Biol. 391 (2009) 498–507. doi:10.1016/j.jmb.2009.05.082.

[60] C. von Ballmoos, P. Dimroth, Two Distinct Proton Binding Sites in the ATP Synthase Family †, Biochemistry. 46 (2007) 11800–11809. doi:10.1021/bi701083v.

[61] A. Krah, D. Pogoryelov, J.D. Langer, P.J. Bond, T. Meier, J.D. Faraldo-Gómez, Structural and energetic basis for H+ versus Na+ binding selectivity in ATP synthase Fo rotors, Biochim. Biophys. Acta - Bioenerg. 1797 (2010) 763–772. doi:10.1016/j.bbabio.2010.04.014.

[62] W. Humphrey, A. Dalke, K. Schulten, VMD: visual molecular dynamics., J. Mol. Graph. 14 (1996) 33–8, 27–8. http://www.ncbi.nlm.nih.gov/pubmed/8744570.

[63] T. Paramo, A. East, D. Garzón, M.B. Ulmschneider, P.J. Bond, Efficient Characterization of Protein Cavities within Molecular Simulation Trajectories: trj_cavity, J. Chem. Theory Comput. 10 (2014) 2151–2164. doi:10.1021/ct401098b.

[64] Y.M. Leung, D.A. Holdbrook, T.J. Piggot, S. Khalid, The NorM MATE Transporter from N. gonorrhoeae: Insights into Drug and Ion Binding from Atomistic Molecular Dynamics Simulations, Biophys. J. 107 (2014) 460–468. doi:10.1016/j.bpj.2014.06.005.

[65] A. Krah, D. Pogoryelov, T. Meier, J.D. Faraldo-Gomez, On the Structure of the Proton-Binding Site in the Fo Rotor of Chloroplast ATP Synthases, J. Mol. Biol. 395 (2010) 20–27. doi:10.1016/j.jmb.2009.10.059.

[66] D.T. Baptista-Hon, A. Krah, U. Zachariae, T.G. Hales, A role for loop G in the β1 strand in GABA A receptor activation, J. Physiol. 594 (2016) 5555–5571. doi:10.1113/JP272463.

[67] D. Pogoryelov, A. Krah, J.D. Langer, Ö. Yildiz, J.D. Faraldo-Gómez, T. Meier, Microscopic rotary mechanism of ion translocation in the Fo complex of ATP synthases, Nat. Chem. Biol. 6 (2010) 891–899. doi:10.1038/nchembio.457.

[68] S. Schulz, M. Iglesias-Cans, A. Krah, Ö. Yildiz, V. Leone, D. Matthies, G.M. Cook, J.D. Faraldo-Gómez, T. Meier, A New Type of Na+-Driven ATP Synthase Membrane Rotor with a Two-Carboxylate Ion-Coupling Motif, PLoS Biol. 11 (2013) e1001596. doi:10.1371/journal.pbio.1001596.

[69] O.N. Vickery, J.-P. Machtens, G. Tamburrino, D. Seeliger, U. Zachariae, Structural Mechanisms of Voltage Sensing in G Protein-Coupled Receptors, Structure. 24 (2016) 997–1007. doi:10.1016/j.str.2016.04.007.

[70] A. Delcour, Outer membrane permeability and antibiotic resistance., Biochim. Biophys. Acta. 1794 (2009) 808–816. doi:10.1016/j.bbapap.2008.11.005.

[71] U. Zachariae, V. Helms, H. Engelhardt, Multistep mechanism of chloride translocation in a strongly anion-selective porin channel., Biophys. J. 85 (2003) 954–62. doi:10.1016/S0006-3495(03)74534-2.

[72] G.D. Wright, Bacterial resistance to antibiotics: enzymatic degradation and modification., Adv. Drug Deliv. Rev. 57 (2005) 1451–70. doi:10.1016/j.addr.2005.04.002.

[73] P.A. Lambert, Bacterial resistance to antibiotics: modified target sites., Adv. Drug Deliv. Rev. 57 (2005) 1471–85. doi:10.1016/j.addr.2005.04.003.

[74] P.S. Stewart, J.. W. Costerton, Antibiotic resistance of bacteria in biofilms., Lancet (London, England). 358 (2001) 135–8. http://www.ncbi.nlm.nih.gov/pubmed/11463434.

[75] G.B. Brandani, M. Schor, R. Morris, N. Stanley-Wall, C.E. MacPhee, D. Marenduzzo, U. Zachariae, The Bacterial Hydrophobin BslA is a Switchable Ellipsoidal Janus Nanocolloid, Langmuir. 31 (2015) 11558–11563. doi:10.1021/acs.langmuir.5b02347.

[76] J.J. Mousa, R.C. Newsome, Y. Yang, C. Jobin, S.D. Bruner, ClbM is a versatile, cation-promiscuous MATE transporter found in the colibactin biosynthetic gene cluster, Biochem. Biophys. Res. Commun. 482 (2017) 1233–1239. doi:10.1016/j.bbrc.2016.12.018.

[77] V. Ngo, M.C. da Silva, M. Kubillus, H. Li, B. Roux, M. Elstner, Q. Cui, D.R. Salahub, S.Y. Noskov, Quantum Effects in Cation Interactions with First and Second Coordination Shell Ligands in Metalloproteins, J. Chem. Theory Comput. 11 (2015) 4992–5001. doi:10.1021/acs.jctc.5b00524.

[78] L. Nie, E. Grell, V.N. Malviya, H. Xie, J. Wang, H. Michel, Identification of the High-affinity Substrate-binding Site of the Multidrug and Toxic Compound Extrusion (MATE) Family Transporter from Pseudomonas stutzeri, J. Biol. Chem. 291 (2016) 15503–15514. doi:10.1074/jbc.M116.728618.